

A SOLVOTHERMAL SINGLE-STEP ROUTE TOWARDS SHAPE-CONTROLLED TITANIUM DIOXIDE NANOCRYSTALS

Cao-Thang Dinh,¹ Thanh-Dinh Nguyen,¹ Freddy Kleitz² and Trong-On Do^{1*}

1. Centre de Recherche sur les Propriétés des Interfaces et la Catalyse (CERPIC), Department of Chemical Engineering, Laval University, Quebec, Canada G1V 0A6

2. Centre de Recherche sur les Matériaux Avancés (CERMA), Department of Chemistry, Laval University, Quebec, Canada G1V 0A6

A versatile synthetic method which is based on a solvothermal technique for the fabrication of highly crystalline TiO₂ nanocrystals (NC) exhibiting different shapes such as rhombic, truncated rhombic, spherical, dog-bone, truncated, and elongated rhombic is reported. The dominant features of the present approach are first the use of water vapor as hydrolysis agent to accelerate the reaction, and second, the use of both oleic acid (OA) and oleylamine (OM) as two distinct capping surfactants having different binding strengths for the control of the growth of the TiO₂ nanoparticles. It is shown that the presence of an appropriate amount of water vapor along with the desired OA/OM molar ratio plays a crucial role in controlling size and shape of TiO₂ NCs. Moreover, it is also established that the thus-obtained TiO₂ NCs are excellent support for the synthesis of composite metal/TiO₂ photocatalysts in which metal clusters are uniformly deposited on the surface of each individual TiO₂ NC.

Keywords: nanocrystals, shape-controlled, titania, photocatalyst, composite nanocrystals

INTRODUCTION

Titanium dioxide nanoparticles (TiO₂ NPs) have attracted great interest owing to their potential application in a wide range of fields such as photocatalysis, dye-sensitive solar cells, photochromic devices, and gas sensing (Fujishima and Honda, 1972; O'Regan and Grätzel, 1991; Barbe et al., 1997; Grätzel, 2001; Chen and Mao, 2007; Rozhkova et al., 2009; Wang et al., 2009). These applications originate from the unique physical and chemical properties of TiO₂ which depend not only on crystal phase and particle size, but also on particle shape (Li and Wang, 2003; Joo et al., 2005; Yang et al., 2008, 2009; Dai et al., 2009; Han et al., 2009). For instance, Joo et al. (2005) demonstrated that TiO₂ nanorods exhibit superior photocatalytic inactivation of *E. coli* than that of conventional Degussa P-25 catalyst. Moreover, changing the shape of the nanocrystals (NCs) allows for more flexibility and provides more modulation of electronic states than by simply changing the size of the particles (Li and Wang, 2003). Controlling over the shape of TiO₂ NPs is therefore of key importance in the fabrication of new advanced materials with desired properties.

Over the past decades, there have been a number of synthetic routes for the preparation of TiO₂ NPs. For instance, conventional

hydrolytic sol-gel process and emulsion precipitation (Murakami et al., 1999; Lin et al., 2002; Sugimoto et al., 2003; Kanie and Sugimoto, 2004) performed at relatively low temperature yield amorphous products with polydisperse particles and subsequent calcination is needed to induce crystallisation. Furthermore, hydrolytic reaction rates are often too high, especially with transition metal precursors, making it difficult to control the processes (Mutin and Vioux, 2009). Because of fast hydrolytic reactions, slight changes in kinetics may lead to dramatic changes in the size and shape of the final materials. Recently, a nonhydrolytic process, which is usually conducted at elevated temperature, was shown to produce monodisperse TiO₂ NPs with high crystallinity (Arnal et al., 1997; Trentler et al., 1999; Hay and Raval, 2001; Niederberger et al., 2002). The use of oxygen-donors other than water under nonhydrolytic conditions results in a drastic decrease in the

*Author to whom correspondence may be addressed.

E-mail address: trong-on.do@gch.ulaval.ca

Can. J. Chem. Eng. 90:8-17, 2012

© 2011 Canadian Society for Chemical Engineering

DOI 10.1002/cjce.20574

Published online 16 May 2011 in Wiley Online Library

(wileyonlinelibrary.com).

reaction rate, thus leading to a slow growth process of particles. Furthermore, for the control of TiO₂ NP morphology, in addition to the control of the reaction rate, the use of surfactants which selectively adsorb on specific particle surfaces has also been shown to play a crucial role (Jun et al., 2003; Zhang et al., 2005; Buonsanti et al., 2008). For example, Jun et al. (2003) reported the synthesis of bullet-, diamond-, and rod-shaped TiO₂ via a nonhydrolytic process, which employed both lauric acid as selective surfactant and trioctylphosphine oxide as nonselective surfactant. However, a relatively low reaction rate of nonhydrolytic reactions compared to that of hydrolytic reactions limits severely the diversity in possible NP morphologies, and as a consequence, few examples of controlled shapes of TiO₂ NPs have been reported so far. Furthermore, efforts have been devoted to combine both hydrolytic and nonhydrolytic reactions in tailoring the size and shape of TiO₂ NPs by adding a certain amount of water to nonaqueous media (Cozzoli et al., 2003; Li et al., 2006; Wu et al., 2008). For instance, Li et al. (2006) used linoleic acid as a capping agent and water produced from the in situ decomposition of NH₄HCO₃ as a hydrolysis agent for the synthesis of TiO₂ NPs. Differently, Wu et al. (2008) prepared rhombic-shaped anatase NCs by using trace amount of water and oleylamine (OM) as hydrolysis agent and capping surfactant, respectively. Nevertheless, the development of facile and reproducible syntheses of shape-controlled TiO₂ NCs with high crystallinity still remains challenging.

Herein, we report a new approach based on solvothermal technique for the tailored synthesis of TiO₂ NCs with controlled shapes, for example, rhombic, truncated rhombic, spherical, dog-bone, truncated and elongated rhombic, and bar. The central features in our approach are the use of water vapor as the hydrolysis agent to accelerate the reaction and the use of both oleic acid (OA) and OM as two distinct surfactants which are commonly used as capping agents in shape controlled synthesis of inorganic NCs (Yin and Alivisatos, 2005; Wang et al., 2007; Dinh et al., 2009) and show different binding strengths to control the growth of the TiO₂ NCs. OA was chosen because the carboxylic acid functional groups are known to tightly bind onto the TiO₂ surface and favour the formation of TiO₂ nanorods (Cozzoli et al., 2003; Joo et al., 2005; Li et al., 2006). OM, on the other hand, was chosen as it was proven effective as surfactant to prepare TiO₂ nanosheets and rhombic-shaped TiO₂ NCs (Wu et al., 2008). Titanium butoxide was chosen as titanium source as it exhibits a low hydrolysis rate owing to longer alkyl group which in turn slows down the diffusion and polymerisation processes (Yoldas, 1986;

Golubko et al., 2001). Slow hydrolysis of titanium butoxide (TB) is clearly favourable in forming TiO₂ NCs with controlled morphology. Herein, we also show that the presence of an appropriate amount of water vapor along with the desired OA:OM molar ratio plays a crucial role in controlling size and shape of TiO₂ NCs. In addition, we demonstrate that these obtained TiO₂ NCs are excellent support for the synthesis of composite metal-TiO₂ NCs in which metal clusters are uniformly deposited on the surface of each individual TiO₂ NC. Ag-TiO₂ NCs were chosen as an example of composite metal-TiO₂ NCs as they combine the advantages of a nontoxic, catalytically active metal showing size- and shape-dependent optical properties and a chemically stable, photoactive and low cost semiconductor material (Ohko et al., 2003; Cozzoli et al., 2004; Zhang et al., 2008; Dinh et al., 2010; Halasi et al., 2010). In addition, interactions between Ag and TiO₂ at the nanoscale could result in new physical properties and enhanced catalytic activity (Ohko et al., 2003).

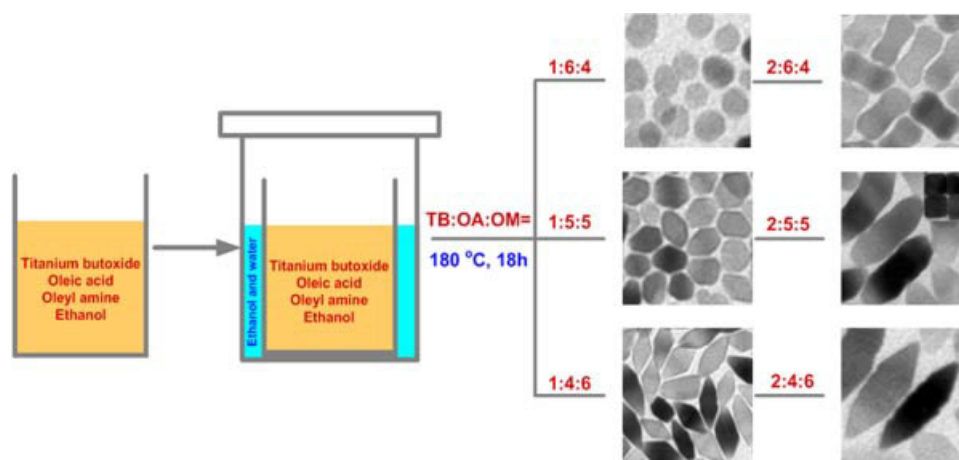
EXPERIMENTAL DETAILS

Chemicals

All chemicals were used as received; silver nitrate (AgNO₃), methylene blue (MB), titanium(IV) butoxide (TB, 97%), OA (90%), and oleyl amine (OM, 70%) were purchased from Sigma-Aldrich Canada Ltd. (Ontario, Canada). Absolute ethanol and toluene solvents were of analytical grade and were also purchased from Aldrich.

Synthesis of TiO₂ NCs

The synthesis of TiO₂ NCs with various shapes was accomplished using a solvothermal method. Typically, TB (5–10 mmol) was added to a mixture of X mmol OA, Y mmol OM, and 100 mmol absolute ethanol (X + Y = 50). X and Y were varied to gain different OA:OM ratios. For example, to synthesise TiO₂ with truncated rhombic shape, 5 mmol of TB was added to a mixture of 25 mmol OA, 25 mmol OM, and 100 mmol absolute ethanol. The obtained mixture in a 40 mL Teflon cup was stirred for 10 min before being transferred into a 100 mL Teflon-lined stainless steel autoclave containing 20 mL of a mixture of ethanol and water (96% v/v ethanol, Scheme 1). The concentration of ethanol was used at the azeotropic point so that the amount of water vapor did not change much during the crystallisation process. The system was then heated at 180°C for 18 h. The obtained white precipitates



Scheme 1. Schematic illustration of the synthesis of TiO₂ nanocrystals with different sizes and shapes.

were washed several times with ethanol and then dried at room temperature. The as-synthesised TiO₂ NP products were then dispersed in nonpolar solvent, such as toluene. To investigate the effect of water on size and shape of resulting TiO₂ NPs, two experiments with pure absolute ethanol and with pure water were also carried out.

Synthesis of Colloidal Ag-TiO₂ Nanocrystals

The as-synthesised TiO₂ NCs were dispersed in toluene followed by the addition of AgNO₃ and ethanol. The obtained mixture was de-aerated with a flow of nitrogen gas and exposed to UV light (365 nm) generated by a 100 W Hg lamp at room temperature. For example, to synthesise Ag-TiO₂ NCs with 2 nm Ag clusters, 5 mmol of as-synthesised TiO₂ NCs were dispersed in 200 mL toluene with no additional OA. AgNO₃ (0.5 g), and ethanol (2 mL) were then added to this solution. The solution was de-aerated by a flow of nitrogen gas for 30 min and then exposed to UV light for 1 min. The resulting mixture was centrifugated to remove undissolved AgNO₃ before ethanol was added to precipitate Ag-TiO₂ NCs. The as-synthesised Ag-TiO₂ NCs powder was washed several times with ethanol in order to remove remaining unreacted AgNO₃.

Characterisation

Transmission electron microscopy (TEM) images and selected area electron diffraction (SAED) of TiO₂ NCs and hybrid Ag-TiO₂ NCs were obtained on a JOEL JEM 1230 operated at 120 kV. Samples were prepared by placing a drop of a dilute toluene dispersion of NCs onto a 200 mesh carbon-coated copper grid and evaporated immediately at ambient temperature. The analysis of the Ag cluster size was carried out by manually digitising the high magnification TEM images with Image Tool. Powder X-ray diffraction (XRD) patterns of the samples were obtained on a Bruker SMART APEXII X-ray diffractometer equipped with a Cu K α radiation source ($\lambda = 1.5418 \text{ \AA}$). X-ray photoelectron spectroscopy (XPS) measurements were carried out in an ion-pumped chamber (evacuated to 10^{-9} Torr) of a photoelectron spectrometer (Kratos Axis-Ultra, Kratos Analytical Ltd., Manchester, United Kingdom) equipped with a focused X-ray source (Al K α , $h\nu = 1486.6 \text{ eV}$). The binding energy of the samples was calibrated by setting the C 1s peak to 285 eV. Peak deconvolution were performed by means of a standard CasaXPS software (v.2.3.13; product of CasaXPS Software Ltd., Teignmouth, United Kingdom) to resolve the separate constituents after background subtraction. The Ag loading content in hybrid Ag-TiO₂ NCs was determined by ICP-MS.

Photocatalysis

Before the photocatalytic tests, the surfactants adsorbed on TiO₂ surface were removed. For the pure TiO₂ NCs, the surfactants were removed as previously reported (Joo et al., 2005). For the composite Ag-TiO₂ NCs, the surfactants were removed by irradiating Ag-TiO₂ NCs dispersed in water for 3 h. The resulting mixture was then centrifugated to obtain a surfactant-free Ag-TiO₂ NCs powder. This powder was dried overnight at 60°C and used as such for photocatalytic test. Photocatalytic activities were evaluated by photocatalytic decomposition of MB. A mixture of MB aqueous solution (20 ppm, 30 mL) and the given photocatalyst (30 mg) was magnetically stirred in absence of light for 30 min to ensure adsorption-desorption equilibrium between the photocatalyst and MB. The mixture was then stirred under UV-Vis irradiation using a 100 W high-pressure Hg lamp. At given time intervals, 3 mL of the suspension was collected and centrifuged

to remove photocatalyst particles. UV-Vis adsorption spectrum of the centrifugated solution was recorded using a Cary 300 Bio UV-Vis spectrophotometer to determine the conversion of the reaction.

RESULTS AND DISCUSSION

Figure 1 shows TEM images of the TiO₂ NPs synthesised with varying OA:OM molar ratio, while leaving the molar ratio of titanium *n*-butoxide (TB) and surfactants unchanged, that is, TB:(OA + OM) = 1:10. The mixture of ethanol and water (96% v/v ethanol) was used for vaporisation. When the OA:OM mole ratio is 4:6, rhombic-shaped TiO₂ NPs with uniform size are obtained (Figure 1A). By increasing the OA:OM molar ratio to 5:5, smaller TiO₂ NCs with truncated rhombic shape are produced (Figure 1B). A further increase of this ratio up to 6:4 leads to the formation of spherical particles with an average size of 13 nm (Figure 1C). One can also point out here that, in all of the cases studied, no large particles were observed and the TiO₂ NPs remained monodisperse in size.

The crystallinity of the synthesised samples was verified by powder XRD. As seen in Figure 2, the XRD patterns of TiO₂ NPs with (a) rhombic, (b) truncated rhombic, and (c) spherical shapes exhibit well-defined peaks assigned to the pure anatase phase (JCPDS File No. 21-1272), indicative of the high crystallinity of these samples. The highly crystalline anatase phase is also revealed by SAED, as shown in Figure 1. The rings can be indexed to diffraction from the (101), (004), (200), (105), (211), and (204) planes of anatase. To confirm the shapes of the obtained TiO₂ NCs, we estimated the average crystallite sizes of anatase NCs by using the Sherrer formula. The average crystallite sizes of rhombic TiO₂ was estimated from the (101) and (004) diffraction peaks using the Sherrer formula to be 18 and 38 nm, respectively. Compared with the TEM images, these two sizes correspond to the width and length of rhombic TiO₂ NCs, respectively. The thickness along the [010] direction of rhombic TiO₂ NCs is difficult to observe by TEM as these NCs have a tendency to lie in the (010) plane (Li et al., 2006; Wen et al., 2007; Wu et al., 2008). However, the thickness can be estimated using the formula $L(010) = 0.364L(211)$, where $L(010)$ is the crystallite size in the [010] direction, corresponding to the thickness of rhombic TiO₂ NCs, and $L(211)$ is the crystallite size obtained from the (211) diffraction peak (Wen et al., 2007). From this formula, the thickness of rhombic TiO₂ NCs is found to be 9.5 nm. In the case of truncated rhombic TiO₂ NCs, the average crystallite sizes estimated from the (004) diffraction peak corresponding to the crystal length, is about 18 nm, in good agreement with the TEM results.

It is established that the formation of TiO₂ undergoes two main steps: (i) hydrolysis of titanium precursors to produce unstable hydroxyalkoxides, and subsequently, (ii) condensation reactions by means ofolation or oxolation to form a Ti-O-Ti network (Livage et al., 1988). The rate of these two processes dramatically affects the shape of the final NC products. In the presence of both water and carboxylic acid, titanium alkoxide can readily react with water or acid (Doeuff et al., 1989; Cozzoli et al., 2003) to form hydroxyalkoxide or carboxyalkoxide, respectively. Subsequently, the reaction between these precursors via a hydrolytic condensation or a nonhydrolytic condensation process produces extensive Ti-O-Ti networks. In general, in the case of titanium, the hydrolytic process is fast, while nonhydrolytic process is comparatively slow (Mutin and Vioux, 2009). Control of the rate of these growth processes is thus essential for tuning the shape evolution of the TiO₂ particles.

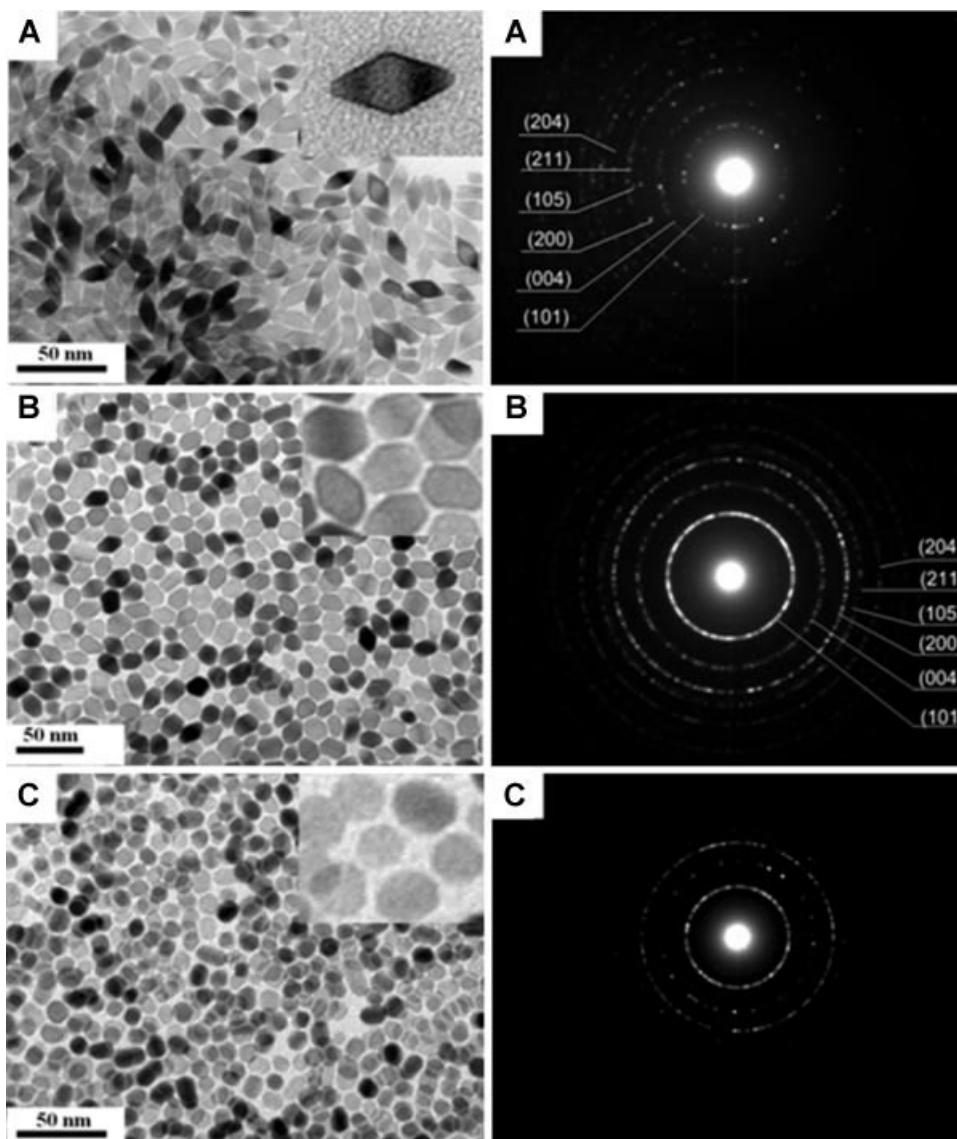


Figure 1. TEM images (left column) and SAED (right column) of TiO₂ NCs with (A) rhombic shape obtained at TB:OA:OM = 1:4:6; (B) truncated rhombic shape obtained at TB:OA:OM = 1:5:5; (C) spherical shape obtained at TB:OA:OM = 1:6:4. Insets show high-magnification images of the corresponding shapes.

In our system, a mixture of ethanol and water was used to generate water vapor which acts as the hydrolysis agent. It is assumed that TB first reacts with water vapor which is generated at elevated temperature to produce hydroxyalkoxide species. This precursor then reacts with OA to form carboxyalkoxide or with other hydroxyalkoxide through hydrolytic condensation as a function of the amount of water and OA used. Note that the formation of carboxyalkoxide is here an important step determining the evolution of TiO₂ crystals. The existence of carboxylic chain can effectively hinder the addition of water at the metal centers. As a result, the hydrolytic condensation is limited. For that reason, the amount of water vapor must have a great influence on the morphology of the TiO₂ particles. To help clarify this point, experiments were carried out to substantiate the effect of water. The TB:OA:OM molar ratio was fixed at 1:6:4, and absolute ethanol or water was used instead of a mixture of ethanol/water. We observed that when ethanol was used alone, monodisperse TiO₂ nanodots were obtained (Figure 3A). In contrast, when only water was used, larger NPs with cubic shape and some aggregated TiO₂ NPs were found (Figure 3B).

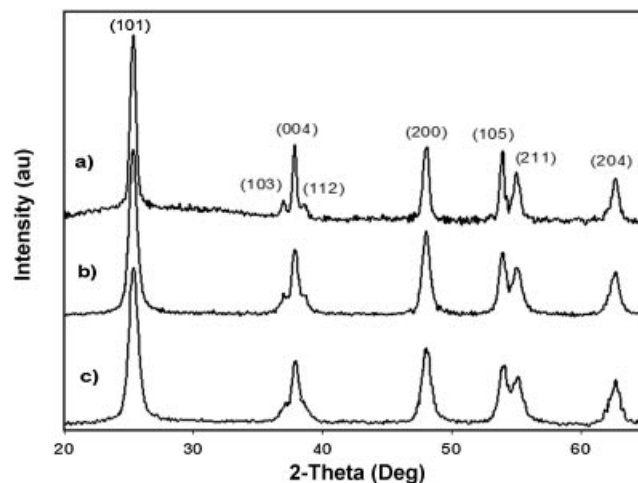


Figure 2. XRD patterns of TiO₂ NCs with (a) rhombic shape obtained at TB:OA:OM = 1:4:6; (b) truncated rhombic shape obtained at TB:OA:OM = 1:5:5; (c) spherical shape obtained at TB:OA:OM = 1:6:4.

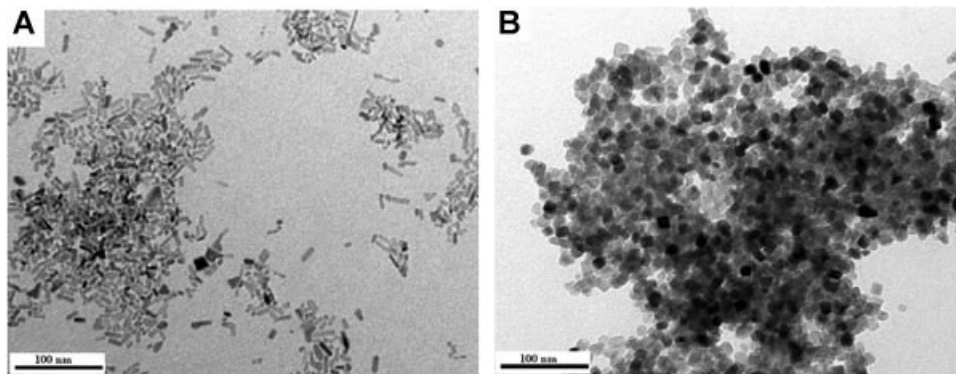


Figure 3. TEM images of TiO_2 nanocrystals obtained (A) with pure ethanol vapor; (B) with pure water vapor (TB:OA:OM = 1:6:4).

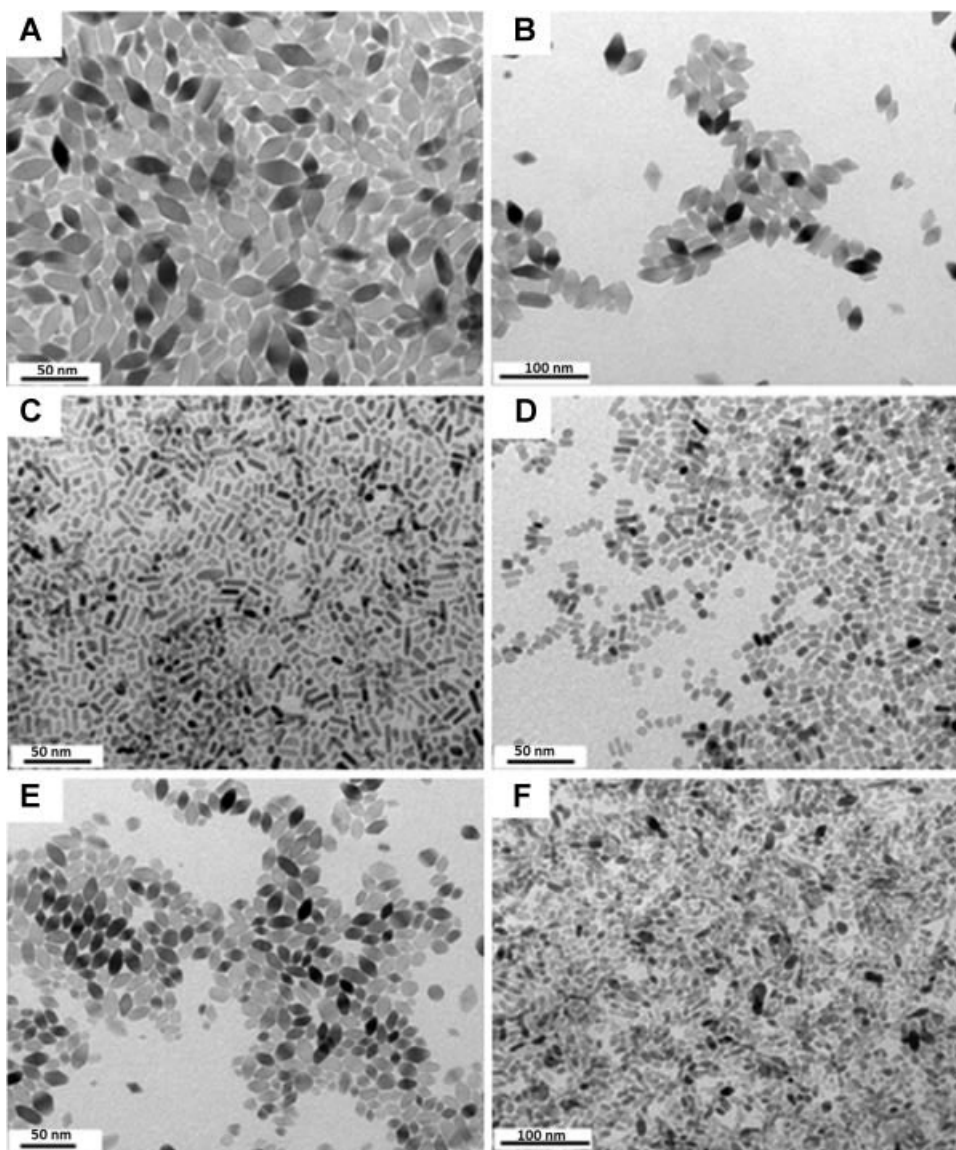
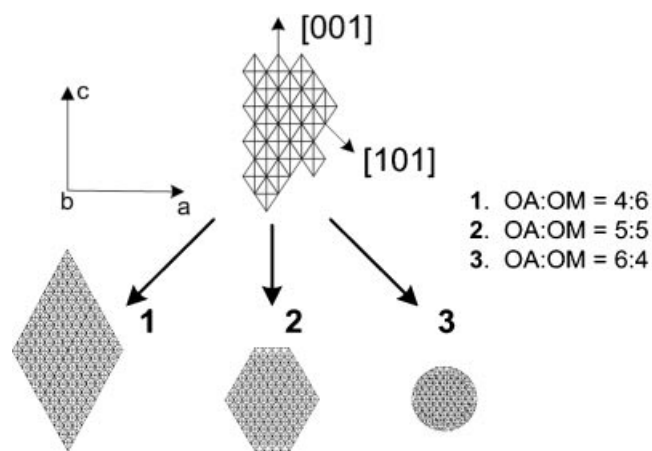


Figure 4. TEM images of rhombic shaped TiO_2 obtained at low OA:OM ratios: (A) TB:OA:OM = 1:2:8 and (B) TB:OA:OM = 1:3:7, TiO_2 nanodots obtained at high OA:OM ratio; (C) TB:OA:OM = 1:8:2 and (D) TB:OA:OM = 1:7:3, TiO_2 nanocrystals obtained using only one surfactant; (E) with OM, TB:OM = 1:5 and (F) with OA, TB:OA = 1:5.

These results indicated that, with a large amount of water, TB reacts vigorously with water through hydrolytic process, leading to the aggregation of the particles. In contrast, in the absence of water, the formation of TiO₂ NCs undergoes slow nonhydrolytic reaction which generally produces nanodots or nanorods (Hay and Raval, 2001; Joo et al., 2005; Zhang et al., 2005).

It is documented that by using surfactants possessing different functional groups with distinct binding strengths, the morphology of resulting particles may be controlled (Ramirez et al., 2004; Mai et al., 2006; Watt et al., 2009). In the case of TiO₂, OA binds strongly to the anatase {001} faces (Jun et al., 2003), whereas OM tends to adhere on the {101} ones (Joo et al., 2005). The selective bindings of these surfactant molecules to different facets of TiO₂ restrict the growth in corresponding direction. In the present system, OA and OM were used not only as capping agents but also as an acid–base pair catalyst, which also contribute to increase condensation rate without affecting hydrolysis rate (Murakami et al., 1999). Moreover, as mentioned above, OA can react with TB or hydroxyalkoxide to generate carboxyalkoxide species which slow down the hydrolytic condensation process. OM, on the other hand, can promote the nonhydrolytic condensation process by aminolysis reaction with titanium carboxylalkoxide (Zhang et al., 2005). It is therefore expected that, by modulating the OA:OM molar ratio, the shape of TiO₂ NCs may be controlled. A series of control experiments was performed with 11 different OA:OM ratios, while keeping the amount of TB and the total surfactant amount constant to elucidate the effect of OA:OM molar ratios to the shape of TiO₂ NPs. The mixture of ethanol and water (96% v/v ethanol) was used for vaporisation. It was found that, when the OA:OM ratio is less than 4:6, only rhombic-shaped TiO₂ NPs are formed (Figure 4A and B). The shape evolution in the range from 4:6 to 5:5 and 6:4 of the OA:OM ratio is further illustrated in Figure 1A–C. When this ratio is higher than 6:4, the NC size decreases markedly, and nanodots of TiO₂ are obtained (Figure 4C and D). Moreover, two additional experiments were also performed using only OA or OM. In the absence of OA, only the rhombic shape was observed, whereas a mixture of spherical particles and nanodots is produced in the absence of OM (Figure 4E and F). These results confirm the cooperative effect of a combination of OA and OM on the resulting particle shapes.

The shape of TiO₂ NCs is determined by the growth rate ratio between the [001] and [101] directions (Chemseddine and Moritz, 1999; Penn and Banfield, 1999). In the absence of OA or at low OA:OM ratio, hydrolytic reactions are predominant, the formation of NPs is thus a fast process. Due to high surface energy of the {001} faces (Donnay and Harker, 1937), growth along [001] is occurring progressively, leading to the depletion of the {001} faces. In contrast, the low surface energy of {101} faces (Donnay and Harker, 1937) and the adhesion of OM to these faces hinder the growth along the [101] direction. As a result, rhombic-shaped TiO₂ NPs are produced (Scheme 2). A similar observation was also reported by Wu et al. (2008) using OM as a capping agent. Increasing the OA:OM ratio slows down the rate of the reaction. The presence of a relative large amount of OA limits the growth along [001] as OA binds selectively to the {001} faces. Consequently, the {001} surfaces is preserved. Crystals grow on both {001} and {101} faces leading to the truncated rhombic or spherical NPs as shown in Figure 1B and C. However, when a large excess of OA is used (OA:OM ratio >6:4), the growth process undergoes nonhydrolytic condensation rather than hydrolytic one. Since OA can adsorb on almost all the surface of TiO₂, the crystals will grow mainly on high surface energy faces (i.e., {001} faces), leading to the formation of nanodots and nanorods.



Scheme 2. Schematic representation showing the shape evolution of TiO₂ NCs as a function of the OA:OM ratio.

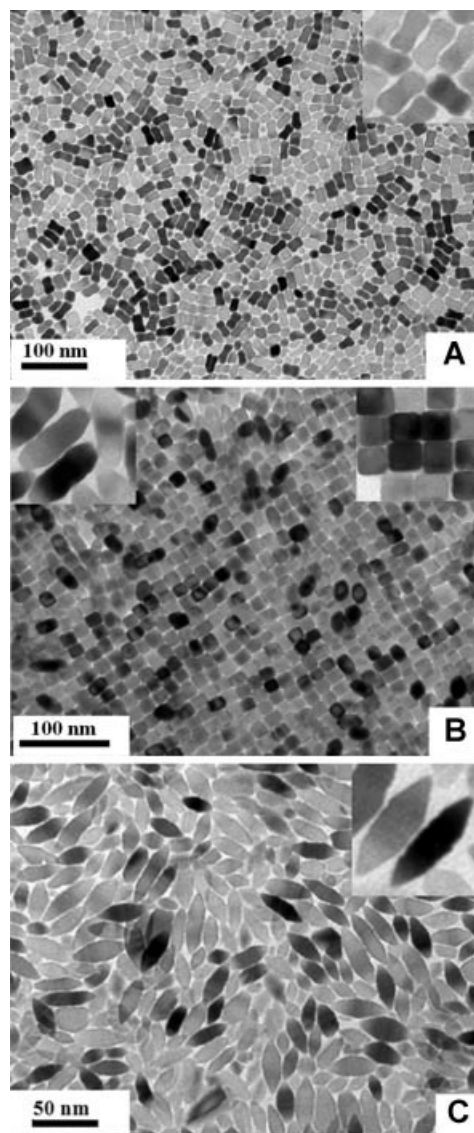


Figure 5. TEM images of (A) dog-bone shaped TiO₂ obtained at TB:OA:OM = 2:6:4; (B) truncated and elongated rhombic TiO₂ obtained at TB:OA:OLA = 2:5:5; and (C) elongated rhombic TiO₂ obtained at TB:OA:OM = 2:4:6.

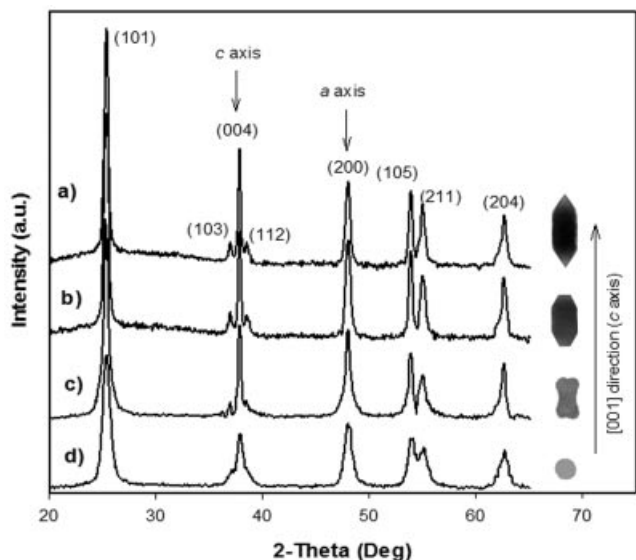


Figure 6. XRD patterns (a) elongated rhombic shaped TiO_2 , (b) truncated and elongated rhombic shaped TiO_2 , (c) dog-bone shaped TiO_2 , and (d) spherical shaped TiO_2 . The XRD pattern of spherical shaped TiO_2 is shown again for comparison.

Previous studies demonstrated that varying the amount of metal precursor also plays an important role in the size and shape evolution of NPs (Peng and Peng, 2001; Nguyen and Do, 2009). We have thus doubled the amount of TB and kept other parameters unchanged, which corresponds to the TB:OA:OM molar ratios of 2:6:4, 2:5:5, and 2:4:6 instead of 1:6:4, 1:5:5, and 1:4:6 (Scheme 1). It was found that when a 2:6:4 ratio was applied instead of

1:6:4, the shape of TiO_2 evolved from spherical (Figure 1C) to uniform dog bone-like particles (Figure 5A). This resulting shape of TiO_2 NCs is to our knowledge found for the first time for TiO_2 NCs. For a ratio of 2:5:5 compared to 1:5:5, a change in the morphology from truncated rhombic (Figure 1B) to elongated and truncated rhombic particles was observed (Figure 5B). The NPs tended to assemble and lie on (001) plane as clearly seen in the inset at right-top corner of Figure 5B. With the 2:4:6 ratio, the formation of elongated rhombic particles was observed (Figure 5C) compared to the rhombic shape obtained with the 1:4:6 ratio.

The powder XRD patterns (Figure 6) of these samples indicated they consist uniquely of the anatase phase. In addition, the (004) diffraction peaks of these three samples appear stronger and sharper, compared to that of spherical TiO_2 , reflecting the evolution along the [001] direction of TiO_2 NPs (Zhang et al., 2005). The elongation of the resulting TiO_2 NCs with increasing the amount of TB may be due to anisotropic crystal growth at high monomer concentration (Peng and Peng, 2001; Lee et al., 2003).

To elucidate the mechanism of formation of the elongated titania particles, we have fixed the OA:OM ratio at 6:4 and gradually increased the amount of TB. Different TB:total surfactant ratios were selected (i.e., TB:total surfactant = 1.3:10, 1.6:10, 2:10, and 4:10). It is found that, with increasing this ratio from 1.3:10 to 1.6:10, the shape of TiO_2 NCs changed from elongated sphere to dumb-bell, as viewed in Figure 7A and B. When the ratio was 2:10, TiO_2 particles with uniform dog-bone shaped were obtained (Figure 7C). However, with further increasing of this ratio to 4:10, the shape of the resulting NCs remained unchanged, but larger and less uniform particles were obtained (Figure 7D). It is worth mentioning that, owing to the polar environment, the surfactant-capped NCs spontaneously precipitated at the bottom of the teflon cup

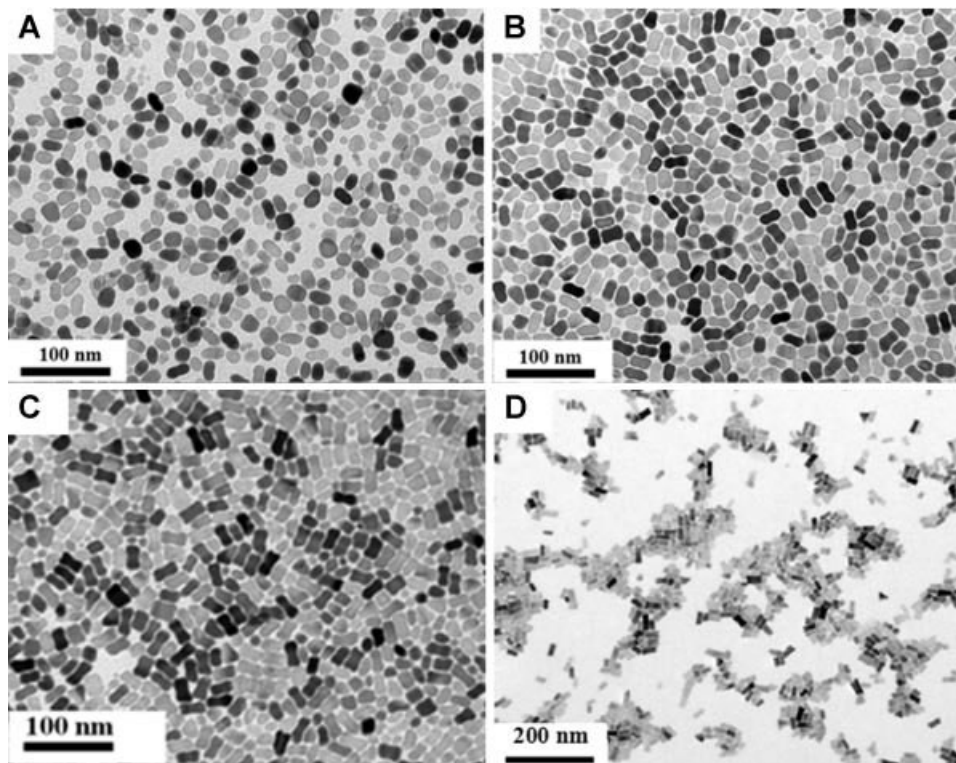


Figure 7. TEM images of (A) elongated spherical TiO_2 obtained at TB:OA:OM = 1.3:6:4; (B) dumb-bell TiO_2 obtained at TB:OA:OM = 1.6:6:4; (C) dog-bone shaped TiO_2 obtained at TB:OA:OM = 2:6:4; and (D) dog-bone shaped TiO_2 obtained at TB:OA:OM = 4:6:4.

as they reached critical size and shape in this kinetically driven regime.

Composite Ag-TiO₂ NCs in which Ag clusters are uniformly deposited on individual TiO₂ NC surface were obtained by using a photodeposition technique in organic solvent (toluene). TiO₂ NC synthesised with TB:OA:OM = 4:5:5 were used as support. Figure 8A and B show representative TEM images of the Ag-TiO₂ NCs synthesised by irradiating a mixture TiO₂ NCs, AgNO₃, and ethanol in toluene for 1 min. As clearly seen, a large number of Ag clusters with uniform size (ca. 2 nm) were well dispersed on the TiO₂ NC surface. In addition, no separated Ag clusters or particles were observed, which implies that Ag clusters grew selectively on the individual TiO₂ NC surface. Importantly, the synthesis solution remained transparent upon irradiation, but the solution colour changed from colourless to light brown indicative of the formation of metallic Ag clusters (inset in Figure 8A). The Ag content in the composite NCs was 2.6 (% mole) as obtained from ICP-MS analyses. Furthermore, the oxidation state of the Ag species was confirmed by XPS. As shown in Figure 9, the Ag 3d_{5/2} peak at a binding energy of 368.0 is characteristic of metallic Ag

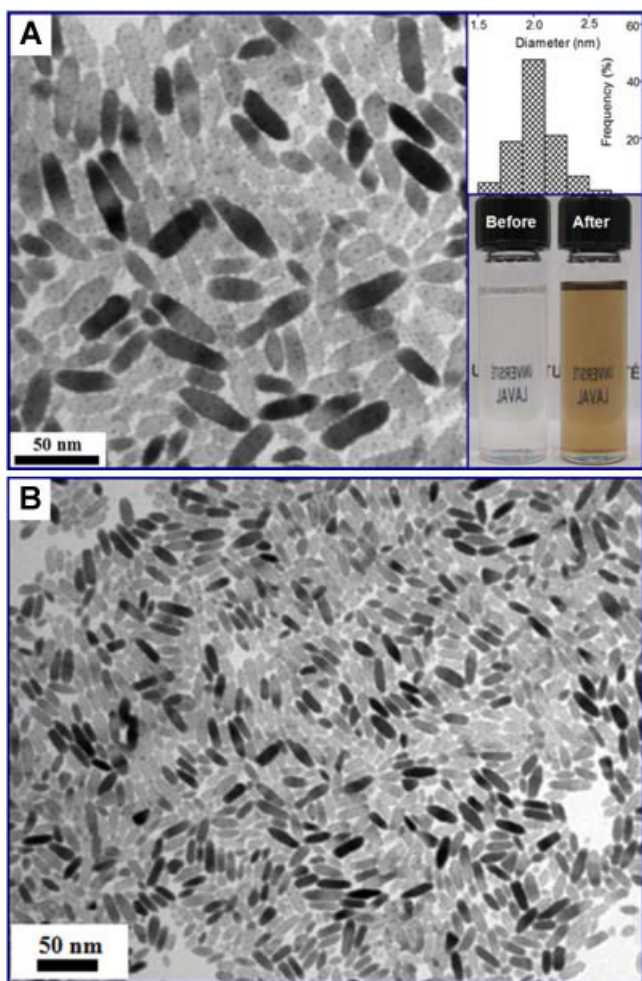


Figure 8. TEM image (A) (high magnification), and (B) (low magnification) of composite Ag-TiO₂ NCs (2.6% mol Ag) synthesised from a solution of TiO₂ NCs containing silver nitrate after UV irradiation (1 min). Insets (A) are size distribution of Ag clusters (upper) and photograph of the Ag-TiO₂ NC solution before and after irradiation (lower). [Color figure can be seen in the online version of this article, available at [http://onlinelibrary.wiley.com/journal/10.1002/\(ISSN\)1939-019X](http://onlinelibrary.wiley.com/journal/10.1002/(ISSN)1939-019X)]

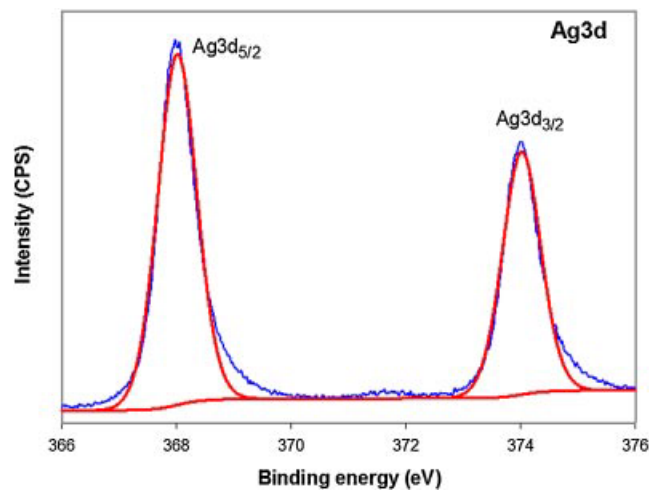
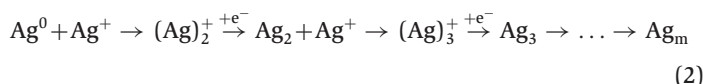
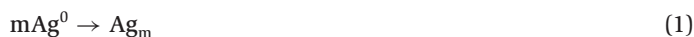


Figure 9. Ag 3d X-ray photoelectron spectrum of the composite Ag-TiO₂ NCs (2.6% mol. Ag) synthesised by irradiating of TiO₂ NCs solution containing silver nitrate salt for 1 min with no additional OA. [Color figure can be seen in the online version of this article, available at [http://onlinelibrary.wiley.com/journal/10.1002/\(ISSN\)1939-019X](http://onlinelibrary.wiley.com/journal/10.1002/(ISSN)1939-019X)]

(Wagner et al., 1979). It is well known that band-gap illumination of TiO₂ creates electron-hole pairs which move to the surface and are consumed for reduction and oxidation reactions (Linsebigler et al., 1995). In our system, the surface electrons both act as reducing agents for conversion of Ag⁺ ions to metallic Ag and as negative charge for attracting Ag⁺ ions to the TiO₂ surface, while the holes are consumed for the oxidation of ethanol or surfactants. Once the metallic Ag atoms are created, Ag clusters on TiO₂ surface can be formed either by aggregation of concurrently formed Ag atoms (Equation 1), or by a sequence of alternating electronic and ionic events as in the photographic process (Equation 2); (Disdier et al., 1983):



However, the presence of surfactants adsorbed on TiO₂ NC surface is expected to hinder the migration of Ag atoms on the TiO₂ surface. Thus, we propose that the latter mechanism by which the size of Ag cluster can be expressed as a function of time is predominant in this case. This mechanism allows us not only to fabricate composite Ag-TiO₂ NCs exhibiting uniform and very small size of Ag clusters, but also to control the size of these clusters without changing their population by simply varying the irradiation time. To evaluate the photocatalytic performance of the new composite Ag-TiO₂ NCs, we selected NCs with Ag clusters of 2 nm and a 2.6% mole Ag loading for the photocatalytic decomposition of MB. For comparison, pure TiO₂ nanorods, commercial P25 and Ag-P25 composites synthesised using the same photodeposition technique with a comparable Ag content (2.8% mole), were also used. Figure 10A shows the spectra of MB solution as a function of time over the hybrid Ag-TiO₂ NCs catalyst. The absorption band at 660 nm, which is characteristic of MB, decreases in intensity with the increase of irradiation time, indicative of the decomposition of MB. As illustrated in Figure 10B, the results indicate that the pure TiO₂ nanorods exhibit a slightly higher catalytic activity than that of P25. This could be due to a shape effect on the

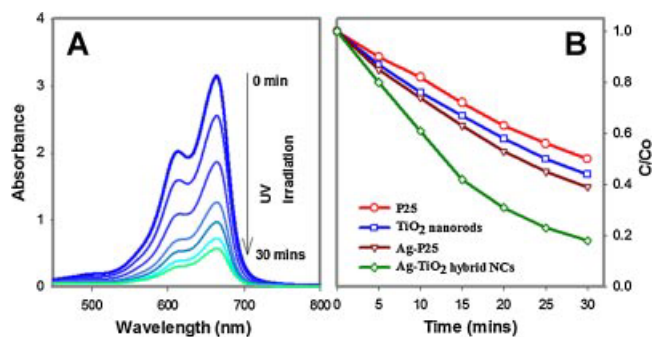


Figure 10. UV-Vis absorption spectra of a methylene blue (MB) solution as a function of irradiation time in the presence of Ag-TiO₂ NCs catalyst (A), and comparison of the MB photodegradation using TiO₂ nanorods, P25, Ag-P25, and Ag-TiO₂ NCs as photocatalysts (B). [Color figure can be seen in the online version of this article, available at [http://onlinelibrary.wiley.com/journal/10.1002/\(ISSN\)1939-019X](http://onlinelibrary.wiley.com/journal/10.1002/(ISSN)1939-019X)]

photocatalytic efficiency (Joo et al., 2005). Both composite Ag-TiO₂ materials show higher photocatalytic activity than that of pure TiO₂ materials. However, the composite Ag-TiO₂ NCs clearly demonstrate a much higher performance for the photocatalytic degradation of MB as compared to Ag-P25. To explain this, we may attribute the high photocatalytic activity of Ag-TiO₂ NCs to a very high dispersion of Ag clusters on the individual TiO₂ NCs.

CONCLUSIONS

This work has demonstrated the possibility of synthesising TiO₂ NCs with various shapes such as rhombic, truncated rhombic, spherical, dog-bone, truncated and elongated rhombic by using a simple solvothermal route which employed both OA and OM as capping agents in the presence of water vapor. In this system, a simple modulation of the OA:OM molar ratio or the amount of TB or reaction temperature enables an unprecedented fine control of the growth rate of TiO₂ NCs, and consequently, a control of the shape of these particles. Such NCs with controlled shape and size will be valuable for further investigating shape-dependent properties of TiO₂. Moreover, the NCs are also excellent supports for the preparation of new composite Ag-TiO₂ NCs which exhibit high catalytic performance in the photodegradation of organic compounds.

REFERENCES

Arnal, P., R. J. P. Corriu, D. Leclercq, P. H. Mutin and A. Vioux, "A Solution Chemistry Study of Nonhydrolytic Sol-Gel Routes to Titania," *Chem. Mater.* **9**, 694-698 (1997).

Barbe, C. J., F. Arendse, P. Comte, M. Jirousek, F. Lenzmann, V. Shklover and M. Grätzel, "Nanocrystalline Titanium Oxide Electrodes for Photovoltaic Applications," *J. Am. Ceram. Soc.* **80**, 3157-3171 (1997).

Buonsanti, R., V. Grillo, E. Carlino, C. Giannini, T. Kipp, R. Cingolani and D. Cozzoli, "Nonhydrolytic Synthesis of High-Quality Anisotropically Shaped Brookite TiO₂ Nanocrystals," *J. Am. Chem. Soc.* **130**, 11223-11233 (2008).

Chemseddine, A. and T. Moritz, "Nanostructuring Titania: Control Over Nanocrystal Structure, Size, Shape, and Organisation," *Eur. J. Inorg. Chem.* **1999**, 235-245 (1999).

Chen, X. and S. S. Mao, "Titanium Dioxide Nanomaterials: Synthesis, Properties, Modifications, and Applications," *Chem. Rev.* **107**, 2891-2959 (2007).

Cozzoli, P. D., A. Kornowski and H. Weller, "Low-Temperature Synthesis of Soluble and Processable Organic-Capped Anatase TiO₂ Nanorods," *J. Am. Chem. Soc.* **125**, 14539-14548 (2003).

Cozzoli, P. D., R. Comparelli, E. Fanizza, M. L. Curri, A. Agostiano and D. Laub, "Photocatalytic Synthesis of Silver Nanoparticles Stabilized by TiO₂ Nanorods: A Semiconductor/Metal Nanocomposite in Homogeneous Nonpolar Solution," *J. Am. Chem. Soc.* **126**, 3868-3879 (2004).

Dai, Y., C. M. Copley, J. Zeng, Y. Sun and Y. Xia, "Synthesis of Anatase TiO₂ Nanocrystals with Exposed {001} Facets," *Nano Lett.* **9**, 2455-2459 (2009).

Dinh, C. T., T. D. Nguyen, F. Kleitz and T. O. Do, "Shape-Controlled Synthesis of Highly Crystalline Titania Nanocrystals," *ACS Nano* **3**, 3737-3743 (2009).

Dinh, C. T., T. D. Nguyen, F. Kleitz and T. O. Do, "A New Route to Size and Population Control of Silver Clusters on Colloidal TiO₂ Nanocrystals," *ACS Appl. Mater. Interfaces* (2010). In press.

Disdier, J., J.-M. Herrmann and P. Pichat, "Platinum/Titanium Dioxide Catalysts. A Photoconductivity Study of Electron Transfer From the Ultraviolet-Illuminated Support to the Metal and of the Influence of Hydrogen," *J. Chem. Soc. Faraday Trans.* **79**, 651-660 (1983).

Doeuff, S., Y. Dromzee, F. Taulelle and C. Sanchez, "Synthesis and Solid- and Liquid-State Characterisation of a Hexameric Cluster of Titanium(IV): Ti₆(μ₂-O)₂(μ₃-O)₂(μ₂-OC₄H₉)₂(OC₄H₉)₆(OCOCH₃)₈," *Inorg. Chem.* **28**, 4439-4445 (1989).

Donnay, J. D. and D. Harker, "A New Law of Crystal Morphology Extending the Law of Bravais," *Am. Mineral* **22**, 446 (1937).

Fujishima, A. and K. Honda, "Electrochemical Photolysis of Water at a Semiconductor Electrode," *Nature* **238**, 37-38 (1972).

Golubko, N. V., M. I. Yanovskaya, I. P. Romm and A. N. Ozerin, "Hydrolysis of Titanium Alkoxides: Thermochemical, Electron Microscopy, Sxas Studies," *J. Sol-Gel Sci Technol.* **20**, 245-262 (2001).

Grätzel, M., "Photoelectrochemical Cells," *Nature* **414**, 338-344 (2001).

Halasi, Gy., A. Kecskeméti and F. Solymosi, "Photocatalytic Reduction of NO With Ethanol on Ag/TiO₂," *Catal. Lett.* **135**, 16-20 (2010).

Han, X., Q. Kuang, M. Jin, Z. Xie and L. Zheng, "Synthesis of Titania Nanosheets With a High Percentage of Exposed (001) Facets and Related Photocatalytic Properties," *J. Am. Chem. Soc.* **131**, 3152-3153 (2009).

Hay, J. N. and H. M. Raval, "Synthesis of Organic-Inorganic Hybrids Via the Non-Hydrolytic Sol-Gel Process," *Chem. Mater.* **13**, 3396-3403 (2001).

Joo, J., S. G. Kwon, T. Yu, M. Cho, J. Lee, J. Yoon and T. Hyeon, "Large-Scale Synthesis of TiO₂ Nanorods Via Nonhydrolytic Sol-Gel Ester Elimination Reaction and Their Application to Photocatalytic Inactivation of *E. coli*," *J. Phys. Chem. B* **109**, 15297-15302 (2005).

Jun, Y. W., M. F. Casula, J.-H. Sim, S. Y. Kim, J. Cheon and A. P. Alivisatos, "Surfactant-Assisted Elimination of a High Energy Facet as a Means of Controlling the Shapes of TiO₂

- Nanocrystals," *J. Am. Chem. Soc.* **125**, 15981–15985 (2003).
- Kanie, K. and T. Sugimoto, "Shape Control of Anatase TiO₂ Nanoparticles by Amino Acids in a Gel–Sol System," *Chem. Commun.* **2004**, 1584–1585 (2004).
- Lee, S.-M., S.-N. Cho and J. Cheon, "Anisotropic Shape Control of Colloidal Inorganic Nanocrystals," *Adv. Mater.* **15**, 441–444 (2003).
- Li, J. and L. W. Wang, "Shape Effects on Electronic States of Nanocrystals," *Nano Lett.* **3**, 1357–1363 (2003).
- Li, X. L., Q. Peng, J. X. Yi, X. Wang and Y. D. Li, "Near Monodisperse TiO₂ Nanoparticles and Nanorods," *Chem. Eur. J.* **12**, 2383–2391 (2006).
- Lin, J., Y. Lin, P. Liu, M. J. Meziani, L. F. Allard and Y. P. Sun, "Hot-Fluid Annealing for Crystalline Titanium Dioxide Nanoparticles in Stable Suspension," *J. Am. Chem. Soc.* **124**, 11514–11518 (2002).
- Linsebigler, A. L., G. Lu and J. T. Yates, Jr., "Photocatalysis on TiO₂ Surfaces: Principles, Mechanisms, and Selected Results," *Chem. Rev.* **95**, 735–758 (1995).
- Livage, J., M. Henry and C. Sanchez, "Sol–Gel Chemistry of Transition Metal Oxides," *Prog. Solid St. Chem.* **18**, 259–341 (1988).
- Mai, H. X., Y. W. Zhang, R. Si, Z. G. Yan, L. D. Sun, L. P. You and C. H. Yan, "High-Quality Sodium Rare-Earth Fluoride Nanocrystals: Controlled Synthesis and Optical Properties," *J. Am. Chem. Soc.* **128**, 6426–6436 (2006).
- Murakami, Y., T. Matsumoto and Y. J. Takasu, "Salt Catalysts Containing Basic Anions and Acidic Cations for the Sol–Gel Process of Titanium Alkoxide: Controlling the Kinetics and Dimensionality of the Resultant Titanium Oxide," *Phys. Chem. B* **103**, 1836–1840 (1999).
- Mutin, P. H. and A. Vioux, "Nonhydrolytic Processing of Oxide-Based Materials: Simple Routes to Control Homogeneity, Morphology, and Nanostructure," *Chem. Mater.* **21**, 582–596 (2009).
- Nguyen, T. D. and T. O. Do, "General Two-Phase Routes to Synthesise Colloidal Metal Oxide Nanocrystals: Simple Synthesis and Ordered Self-Assembly Structures," *J. Phys. Chem. C* **113**, 11204–11214 (2009).
- Niederberger, M., M. H. Bartl and G. D. Stucky, "Benzyl Alcohol and Transition Metal Chlorides as a Versatile Reaction System for the Nonaqueous and Low-Temperature Synthesis of Crystalline Nano-Objects With Controlled Dimensionality," *J. Am. Chem. Soc.* **124**, 13642–13643 (2002).
- O'Regan, B. and M. Grätzel, "A Low-Cost, High-efficiency Solar Cell Based on Dye-sensitized Colloidal TiO₂ Films," *Nature* **353**, 737–740 (1991).
- Ohko, Y., T. Tatsuma, T. Fujii, K. Naoi, C. Niwa, Y. Kubota and A. Fujishima, "Multicolour Photochromism of TiO₂ Films Loaded With Silver Nanoparticles," *Nat. Mater.* **2**, 29–31 (2003).
- Peng, Z. A. and X. Peng, "Mechanisms of the Shape Evolution of CdSe Nanocrystals," *J. Am. Chem. Soc.* **123**, 1389–1395 (2001).
- Penn, R. L. and J. F. Banfield, "Morphology Development and Crystal Growth in Nanocrystalline Aggregates Under Hydrothermal Conditions: Insights From Titania," *Geochim. Cosmochim. Acta* **63**, 1549–1557 (1999).
- Ramirez, E., S. Jansat, K. Philippot, P. Lecante, M. Gomez, A. M. Masdeu-Bulto and B. Chaudret, "Influence of Organic Ligands on the Stabilisation of Palladium Nanoparticles," *J. Organomet. Chem.* **689**, 4601–4610 (2004).
- Rozhkova, E. A., I. Ulasov, B. Lai, N. M. Dimitrijevic, M. S. Lesniak and T. A. Rajh, "High-Performance Nanobio Photocatalyst for Targeted Brain Cancer Therapy," *Nano Lett.* **9**, 3337–3342 (2009).
- Sugimoto, T., X. Zhou and A. Muramatsu, "Synthesis of Uniform Anatase TiO₂ Nanoparticles by Gel–Sol Method: 4. Shape Control," *J. Colloid Interface Sci.* **259**, 53–61 (2003).
- Trentler, T. J., T. E. Denler, J. F. Bertone, A. Agrwal and V. L. Colvin, "Synthesis of TiO₂ Nanocrystals by Nonhydrolytic Solution-Based Reactions," *J. Am. Chem. Soc.* **121**, 1613–1614 (1999).
- Wagner, C. D., W. M. Riggs, L. E. Davis and J. F. Moulder, "Handbook of X-Ray Photoelectron Spectroscopy," Perkin-Elmer Corp., Physical Electronics Division, Eden Prairie, MN (1979).
- Wang, X., Q. Peng and Y. Li, "Interface-Mediated Growth of Monodispersed Nanostructures," *Acc. Chem. Res.* **40**, 635–643 (2007).
- Wang, D., D. Choi, J. Li, Z. Yang, Z. Nie, R. Kou, D. Hu, C. Wang, L. V. Saraf, J. Zhang, I. A. Aksay and J. Liu, "Self-Assembled TiO₂–Graphene Hybrid Nanostructures for Enhanced Li-Ion Insertion," *ACS Nano* **3**, 907–914 (2009).
- Watt, J., N. Young, S. Haigh, A. Kirkland and R. D. Tilley, "Synthesis and Structural Characterisation of Branched Palladium Nanostructures," *Adv. Mater.* **21**, 2288–2293 (2009).
- Wen, P. H., H. Itoh, W. P. Tang and Q. Feng, "Single Nanocrystals of Anatase-Type TiO₂ Prepared From Layered Titanate Nanosheets: Formation Mechanism and Characterisation of Surface Properties," *Langmuir* **23**, 11782–11790 (2007).
- Wu, B. H., G. Y. Guo, N. F. Zheng, Z. X. Xie and G. D. Stucky, "Nonaqueous Production of Nanostructured Anatase With High-Energy Facets," *J. Am. Chem. Soc.* **130**, 17563–17567 (2008).
- Yang, H. G., C. H. Sun, S. Z. Qiao, J. Zou, G. Liu, S. C. Smith, H. M. Cheng and G. Q. Lu, "Anatase TiO₂ Single Crystals With a Large Percentage of Reactive Facets," *Nature* **453**, 638–641 (2008).
- Yang, H., G. Liu, S. Qiao, C. Sun, Y. Jin, S. C. Smith, J. Zou, H. M. Cheng and G. Q. Lu, "Solvothermal Synthesis and Photoreactivity of Anatase TiO₂ Nanosheets With Dominant {001} Facets," *J. Am. Chem. Soc.* **131**, 4078–4083 (2009).
- Yin, Y. and A. P. Alivisatos, "Colloidal Nanocrystal Synthesis and the Organic–Inorganic Interface," *Nature* **437**, 664–670 (2005).
- Yoldas, B. E., "Hydrolysis of Titanium Alkoxide and Effects of Hydrolytic Polycondensation Parameters," *J. Mater. Sci.* **21**, 1087–1092 (1986).
- Zhang, Z., X. Zhong, S. Liu, D. Li and M. Han, "Aminolysis Route to Monodisperse Titania Nanorods With Tunable Aspect Ratio," *Angew. Chem. Int. Ed.* **44**, 3466–3470 (2005).
- Zhang, H., G. Wang, D. Chen, X. Lv and J. Li, "Tuning Photoelectrochemical Performances of Ag–TiO₂ Nanocomposites Via Reduction/Oxidation of Ag," *Chem. Mater.* **20**, 6543–6549 (2008).

Manuscript received November 1, 2010; revised manuscript received February 14, 2011; accepted for publication March 3, 2011.